RGB-NIR Active Gated Imaging

Authors: Nick Spooren[1], Bert Geelen[1], Klaas Tack[1], Andy Lambrechts[1], Murali Jayapala[1], Ran Ginat[2], Yaara David[2], Eyal Levi[2], Yoav Grauer[2]

[1] imec VZW, Kapeldreef 75, B-3001 Leuven, Belgium
[2] BrightWay Vision LTD, Adv. Tech. Center, P.O.B 15126, Haifa 3190500, Israel

ABSTRACT

This paper presents multispectral active gated imaging in relation to the transportation and security fields. Active gated imaging is based on a fast gated camera and pulsed illuminator, synchronized in the time domain to provide range based images. We have developed a multispectral pattern deposited on a gated CMOS Image Sensor (CIS) with a pulsed Near Infrared VCSEL module. This paper will cover the component-level description of the multispectral gated CIS including the camera and illuminator units. Furthermore, the design considerations and characterization results of the spectral filters are presented together with a newly developed image processing method.

Keywords: Active Gated Imaging System (AGIS), Gated CMOS Imager Sensor (GCMOS), VCSEL, Multispectral Imaging, Transportation and Security.

1. INTRODUCTION

In recent years, much effort has been devoted to the development of a single image sensor camera, able to capture images in all weather and light conditions in a cost-effective approach. Today, a large variety of imaging technologies are available on the market, operating from the visible spectrum up to the Far Infrared and even beyond (such as millimeter wave radiation). CMOS based imaging is the way to go in many sectors including transportation, security and commercial. CMOS image sensor technology is progressing rapidly in terms of pixel sensitivity, pixel pitch and versatility of pixel/image sensor architectures. However, the most important feature of CMOS image sensor is the affordability and declining price as the technology continues to mature.

When dealing with safety and security (outdoor) applications low light and wide dynamic ranges are of utmost importance. A common approach in existing state-of the art active imaging is to use a High Dynamic Range (HDR) camera combined with continuous Near Infra-Red (NIR) light sources. Active imaging with constant illumination can provide good contrast and high resolution images in total darkness, but suffers from backscattering effects that significantly degrade the performance in harsh weather conditions. In addition, this method lacks the ability to resolve the power density loss as a function of the range (i.e. inverse-square illumination law) [1]. Another possibility is to use the more traditional combination of a visible and NIR camera to cope with outdoor harsh environments. However, none of these approaches assure any significant improvement of visibility in day to day scenario with

- Low ambient light conditions
- Intense ambient light conditions
- Harsh weather conditions (e.g. rain, snow, smog)

As part of the Horizon 2020 Framework, a program of the European Union, the I-ALLOW project [1] aims to demonstrate a cost-effective novel imaging and detection system based on multispectral active gated imaging technology to resolve these problems. This paper covers some of the core technical aspects of this project. The system consists of:

- A novel, Gated CMOS Image Sensor (GCMOS)
- Novel spectral filters, monolithically integrated on top of the GCMOS image sensor
- A Vertical Cavity Surface Emitting Laser (VCSEL) module emitting in the NIR spectral region.

Electro-Optical and Infrared Systems: Technology and Applications XIII, edited by David A. Huckridge, Reinhard Ebert, Stephen T. Lee, Proc. of SPIE Vol. 9987, 998704 · © 2016 SPIE
CCC code: 0277-786X/16/$18 · doi: 10.1117/12.2239603

We believe that these integrated modules provide the best outdoor imaging solution with a cost effective approach.

Active gated imaging has the benefits of a constant active-illumination method, with the additional abilities of imaging in harsh weather conditions. Range-gating is based on the acquisition of several time of flight events to acquire slices at the desired depth of field. Furthermore, it provides an image of unified signal as a function of the depth of field. Targeting ranges of dozens to hundreds of meters, correlates to light pulses with temporal widths in the order of microseconds. Even with high power illumination, the amount of signal per pulse can be as low as several photons, thus the Signal to Noise Ratio (SNR) that can be achieved from such a pulse, is quite low. In order to enable good SNR, many pulses need to be accumulated. Multi pulse gating enables improving the image's SNR by accumulating the signals of many pulses. Regular sensors are designed for a single integration per frame, thus they do not support this mode of operation. Therefore, a GCMOS image sensor was developed to enable multi-integration for a single image frame, with low noise per gate (or sub-exposure), in order to preserve the low noise levels even with hundreds or more gates/pulses. It also has a fast switching time (implemented on the pixel level) that supports the fast gating, and is optimized for NIR high quantum efficiency.

The standard GCMOS-based Active Gated Imaging System (AGIS) has a narrow Band Pass Filter (BPF) that transfers mainly the wavelengths of the illumination source [3]-[6]. This configuration lacks the visible spectrum that is desired for certain image processing / computer vision functions and for display enhancement applications. In this project, the NIR filter and additional visible filters were integrated on the gated pixel array. The type of filters chosen were a BPF, similar in electro-optical parameters to the one used in the standard system and red (R), green (G) and blue (B) color filters, so color reproduction would be easier. In order to maintain a high NIR resolution, a checker board pattern using half of the pixels was used. The RGB pattern on the remaining half of the pixels uses the same ratio as a regular RGB imager, with half of the pixels with a green filter, and the red and blue with a quarter each. Similar patterns were produced commercially, in sensors like TRUESENSE by OnSemi [10] where the RGB pixels were arranged in a scaled GRGB pattern [7]. We designed the pattern differently, in order to distribute the RGB pixels evenly, thus optimizing the color sample resolution.

Standard RGB absorption filters used in RGB image sensors exhibit significant leakage in the NIR spectral range. This leakage is typically removed by implementing a NIR rejection filter at lens-level. However, if we want to capture information in this spectral range a system level NIR rejection is not adequate. Integrating two interference filters at pixel-level addresses this issue. One interference filter (BPF) is sensitive to the NIR spectral-range and is placed at the positions specified by IR in Figure 1. The second interference filter (short-pass filter) blocks the NIR spectral range and is placed at the locations of the RGB pixels to remove the leakage of the RGB color filters. The absorption-based RGB color filters are deposited on top of the NIR blocking filters, after the deposition and patterning of both interference filters. This way the RGB pixels only capture the visible spectrum.

The pixel-level monolithic integration of optical interference filters on top of the GCMOS image sensor enables the production of a low-cost and very compact RGB/NIR vision system. The integration of optical interference filters has previously been demonstrated in [8]- [10]. In this paper we present the design and first experimental results of two different interference filters, a NIR bandpass filter and a NIR blocking filters. These filters will be monolithically integrated on pixel level using a novel deposition process. The system captures both the information from the standard RGB channels and from the NIR channel corresponding to the light emitted by the NIR pulsed-light source, based on a Vertical Cavity Surface Emitting Laser (VCSEL) module. The transmission of these integrated interference filters is highly customizable, therefore the spectral response of the integrated filter, is not limited to the NIR regime reported in this paper.

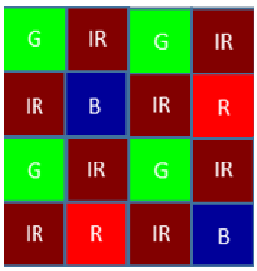

Figure 1: Filter pattern on top of the GCMOS image sensor.

The desired illumination source is required to operate in a wide range of operating temperatures, to have a high efficiency and to have a narrow emission spectrum. In addition, the peak output power should be in the order of several hundreds of watts and the source should be cost effective. LEDs are relatively cost effective, but they have a wide emission spectrum and limited peak power. High power edge emitters suffer from strong wavelength shift with temperature of around 0.3nm/K and usually have a limited range of operating temperatures. The chosen illuminator is based on VCSELs, since they typically exhibit a low wavelength shift with temperature in the order of 0.065nm/K, a highly uniform beam profile and high efficiency of over 40% over a wide temperature span. Importantly they provide a cost-effective solution for high power applications and are convenient for scaling.

In Section 2 the GCMOS image sensor system will be explained and the requirements on its key components are given. Section 3 describes performance of the designed interference filters (NIR BPF and NIR blocking filter) and the design procedure. Section 4 gives a high level description of the newly developed image processing flow and section 5 presents the results of the characterization of the interference filters on top of blank wafers. Finally, section 6 presents the conclusions of this paper.

2. ACTIVE GATED IMAGING SYSTEM DESCRIPTION

Active gated-imaging technology incorporates a range-gating technology, based on multiple "Time-of-Flight" events per single read-out image frames, in the sensor.

Active gating technology combines two key components: a pulsed light source (i.e. laser, LED) and a specially designed gated-sensor that exposes and blocks light at high speeds (in the order of 0.01-2 μs). Each reflected light source pulse is accumulated in the gated-sensor based on a specific "Time-of-Flight" event. Once a desired signal (corresponding to a desired depth-of-field) is accumulated in the sensor, the image is read-out. This method provides high SNR with relatively low peak power illumination.

2.1 Active Gated Imaging System

Figure 2 depicts the system block diagram comprising two main modules; a camera unit and an illuminator unit (i.e. light source). The block diagram describes the proposed system exploiting a common hardware and processing infrastructure.

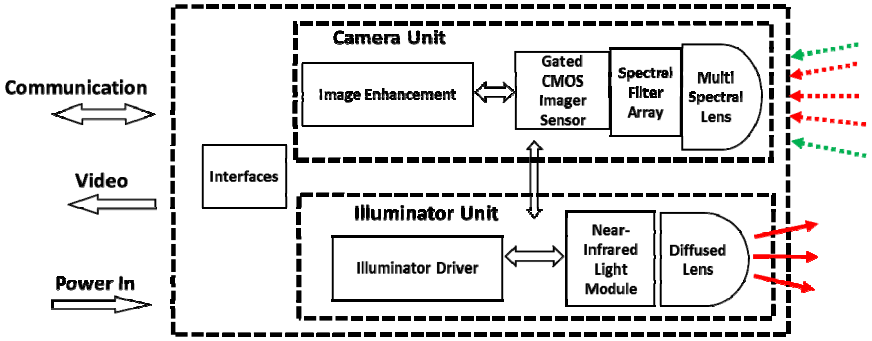

Figure 2: System Block Diagram.

2.2 Active Gated Imaging Modules

The camera unit consists of a dedicated gated-image sensor (GCMOS), fabricated in 0.18μm CMOS technology [11]. GCMOS has three operating modes within a single image frame: single exposure mode, repetitive exposure mode and standard mode. The GCMOS pixel array exposure is synchronized to a single illumination pulse in single mode operation. In repetitive exposure mode, each GCMOS pixel array exposure is synchronized to each illumination pulse, in a single image frame. In contrast with the single exposure and repetitive exposure operation modes, GCMOS pixel array exposure is not synchronized to the system illumination scheme in standard mode.

GCMOS provides:

- For single / repetitive exposure mode: High efficiency per exposure in a single image frame (which is read-out of the imager sensor)

- High anti-blooming ratio (above 5,000) between adjacent pixels
- High shutter efficiency (i.e. high opaqueness during non-gate time)
- High sensitivity in the NIR, above 40% quantum efficiency (QE x fill factor).

An optical design provides the required field-of-view by an objective lens (preferably an image-side tele-centric lens design), with a wide spectral band (400-900nm). A real-time processor handles system control, image enhancement and image processing.

The Illuminator unit consists of a laser module in the NIR spectrum, preferably a diode laser, due to the following considerations:

- Limited temperature induced wavelength shifts as compared to LEDs
- High uniformity of beam profile
- Convenient for rescaling (i.e. based on the number of emitters)
- Compliance to camera surveillance requirements (i.e. environmental, reliability, etc.)

A laser is preferred over other means of illumination such as LED, flash lamp, etc. due to its narrow spectral width (on the order of several nm), high peak power (on the order of a few hundred watts) and high efficiency (above 40%). The laser module is driven by a controller providing synchronization of each laser pulse to each camera exposure (gate). A diffused optical design provides the required illumination, angular distribution and optical power distribution. The Illuminator unit should fulfill laser safety standards such as IEC 60825 and may be calculated as has previously been demonstrated in [12].

System parameters are noted in Table 1.

Table 1. System main parameters.

Camera Unit	
CIS type	GCMOS
Operating modes	• Synchronized to an active pulsed light source: o Single exposure mode o Repetitive exposure mode • Standard mode such as global shutter
Gated image sensor single exposure duration	0.01-2 μs
Gated image sensor resolution	1280 X 960 pixels
Frame rate	120FPS
Illuminator Unit	
Laser type	VCSEL
Operating method	Repetitive pulses with a very low overall duty cycle
Central Wavelength	808 nm
Single pulse duration	0.01-2 μs
Average optical power	Less than 5Watt
Field-of-Illumination	Extended diffused source with large divergence angles

3. PIXEL LEVEL INTEGRATION OF INTERFERENCE FILTERS

In order to simultaneously capture both the RGB color and NIR information with a GCMOS a pixel level integration of the spectral filters is needed. Monolithic pixel-level integration of Fabry-Pérot based interference filters, has been successfully demonstrated in [8]-[10] which present the performance of novel compact CMOS-based hyperspectral camera architectures. The spectral filters in these systems are integrated on top of standard, off-the-shelve, CMOS sensors. The use of CMOS process technology heavily reduces the cost and improves the compactness of these hyperspectral cameras. Additionally, monolithic integration of the filters reduces the stray light in the system. In this paper we adopt some of the filter deposition techniques described in [8]-[10] to enable the extension of the spectral range

used in standard RGB cameras towards NIR. The interference filters will be combined with conventional absorption based RGB filters to have a good color discrimination.
The spectral response of thin film interference filters is sensitive to the angle of incidence of the light. Therefore, the filters were designed considering the system-level performance of the sensor, including the interaction with the objective lens. The objective lens used in our system has a F/# of 1.2, which corresponds to a cone half angle of approximately 24.6º. This low F/# of the objective lens maximizes the irradiance captured by the sensor during night-time conditions. In addition, the maximal Chief Ray Angle (CRA) of the system was specified to be 19º, which is linked to the captured field of view. The filters were designed in such a way that the effect of the angularity of the incident light on the filter response was minimized.

The filters were designed and simulated using the commercially available thin film design software TFCalc [13].

3.1 NIR BPF

The NIR filter was designed to transmit the reflections of the VCSEL wavelength illumination on the surroundings captured by the GCMOS image sensor. To enable a thermally stable operation of the camera unit the NIR BP filter should be able to capture the laser signal at different operating temperatures. The thermally induced spectral drift of the laser module will impose the minimum required Full-Width Half-Maximum (FWHM) of the BP filter. Figure 3 shows the simulated output spectrum of a typical VCSEL with a 1.5nm FWHM and a temperature induced wavelength shift of 0.065 nm/K. The used target for the FWHM during the design of the filter was 35 nm.

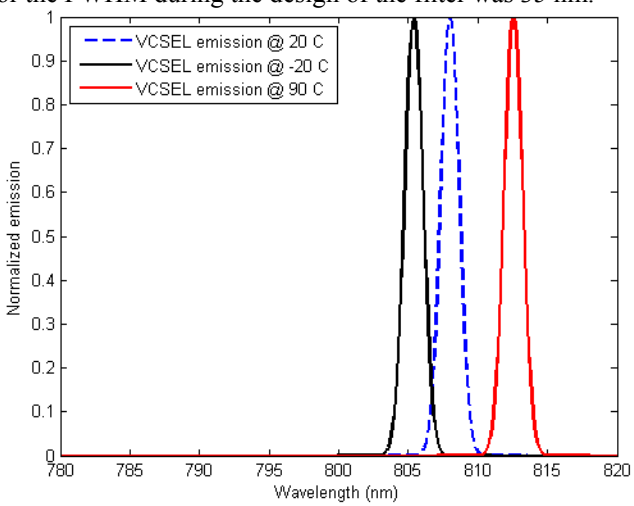

Figure 3: VCSEL emission spectrum at several operating temperatures.

The center of the filter was designed to be around 808 nm, which is the central wavelength of the VCSEL module operating at room temperature. The design of the selected filter is based on a double cavity Fabry-Pérot thin film interferometer. The optical stack was optimized for the F/# of the objective lens and the angular variation of the incident rays across the sensor.

The transmittance of the final design is shown in Figure 4. The response of the filter for ortho-collimated light is shown by the black solid line, while the blue dotted curve shows the impact of the objective lens on the response of the filter. Finally, the red dotted curve shows the combined effect of the objective lens and an incident angle of 12º on the transmittance of the filter.

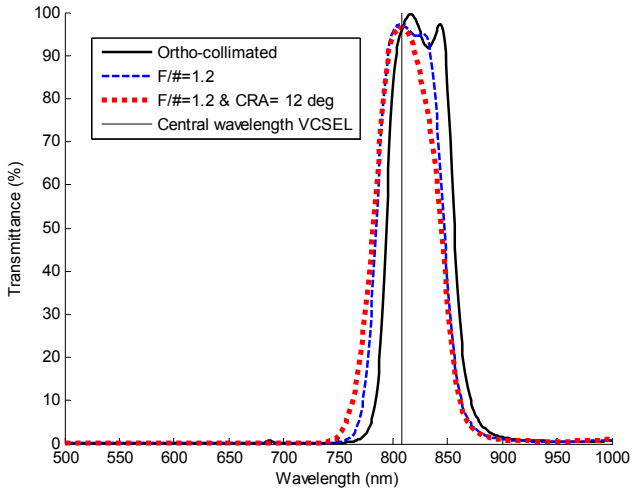

Figure 4: Transmittance as a function of wavelength for the final filter design. The black curve depicts the transmittance of the filter when illuminated by ortho-collimated incident light. The blue curve shows the response when considering the objective lens with F/# equal to 1.2. Finally, the red curve corresponds to the response of the filter where the chief ray angle (CRA) is equal to 12º.

Figure 4 shows a spectral shift of the NIR filter towards shorter wavelengths caused by the objective lens in front of the filter (blue dotted curve). The dotted curves are obtained from a weighted average of the response at different angles all within the cone half angle originating from the objective lens. Table 2 gives the transmission of the filter at the lasing wavelength of the VCSEL module (808 nm) and its FWHM. Note, the transmission efficiency is higher for the response to a cone angle originating from a lens with F/# 1.2. This is due to the optimization procedure which took into account the cone angle. Between the edge and the center of the sensor the transmission of the filter at 808 nm still exceeds the response for collimated light. This shows that our design is very robust towards variations of the angularity of the incident light. In addition, the FWHM of the filter does not vary significantly under non-normal incidence. The FWHM of the filter is wider than set by the specifications, however the filter is still able to capture the light when operating in the specified temperature range. In conclusion, this filter design is compliant with the specifications set by the full system.

Table 2: Transmission properties of the NIR filter for the different angularities of illumination.

Angularity	**Transmission (808 nm)**	**FWHM**	**Out of Band blocking (Average Optical Density)**	
			500-750 nm	**900-1000 nm**
Ortho-collimated	94 %	62.2 nm	4.3	2.2
F/#=1.2	97.7 %	62.8 nm	4.3	2.2
F/#=1.2 & CRA = 12º	97.2 %	63.4 nm	4.2	2.2

3.2 NIR Blocking Filter

The GCMOS image sensor with monolithically integrated filters is able to do parallel acquisition of both the standard RGB channels and an additional NIR channel. This parallel acquisition is enabled by the pixel level integration of an additional NIR blocking filter for the RGB color filters. The NIR blocking filter should transmit the light covering the spectral range of the RGB filters, while blocking the NIR spectral range especially at 808 nm. The minimum average transmission required within the passband is 60 %. The targeted cutoff wavelength of the blocking filter was 700 nm with an allowed deviation of ± 3%. The design of this low pass filter is based on an optimized Bragg stack configuration. The transmission curves of the filter corresponding to different illumination angularities are shown in Figure 5. The black solid curve corresponds to the transmission of the blocking filter, when illuminated by ortho-collimated light. The blue dotted curve shows the response of the filter when taking the objective lens of the system into account. This curve is

the weighted average response of the filter for the different source angles within the light cone imposed by the relative aperture of the lens. Finally, the red dotted curve depicts the response of the filter at CRA=12º in combination with an F/1.2 objective lens.

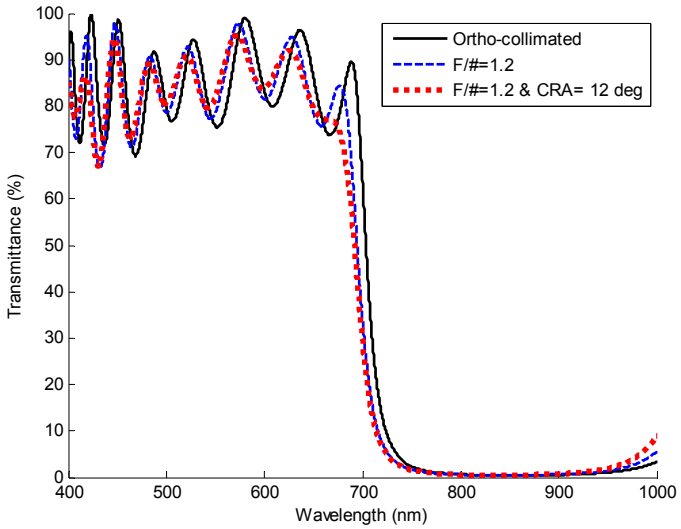

Figure 5: Transmittance as a function of wavelength for the NIR blocking filter. The black curve is the response for collimated light, the blue curve corresponds to the effect of the objective lens and the red filter shows the effect of the objective lens and the CRA.

As explained, it is important that the NIR blocking filter has a good rejection of light at the wavelength of the VCSEL module (808 nm). The Optical Density (OD) at 808 nm of the NIR rejection filter, is shown in

Table 3 for the different illumination angularities. The average OD does not change significantly when changing the angle of incidence. When considering the objective lens, the OD of the filter at 808 nm is equal to 2.3, both at the center and edge of the sensor. This value corresponds to a transmittance of 0.5%. Additionally,

Table 3 shows the variation of the cutoff wavelength and average transmittance in the passband of the filter. When considering the objective lens, the cutoff wavelength of the filter is located at 694.5 nm and the average transmission within the passband is 83.8 %. For every configuration the average transmission within the passband exceeds the set target of 60%. Additionally, the edge wavelength is located within the range set by the specifications, 700 nm (± 3%).

Table 3: Optical density of the NIR blocking filter at 808 nm, for different illumination angularities.

Angularity	Optical Density (808 nm)	Cutoff wavelength	Average Transmittance (Passband)	Average Optical Density (700-1000 nm)
Ortho-collimated	2.2	703.4 nm	84.3 %	1.9
F/#=1.2	2.3	694.5 nm	83.8 %	1.9
F/#=1.2 & CRA = 12º	2.3	691.8 nm	83.2 %	1.9

4. IMAGE PROCESSING FLOW

As with every common color camera, we need to design an algorithm that will take the 2D Color Filter Array (CFA) image and transform it to a 3D image in the RGB color space (this process is known as demosaicing) [14]-[18]. However, in our case, we have a fourth channel in the CFA which can be very different from the other three channels, though it is mostly correlated with them. As the spatial resolution of the NIR channel sampling is much higher than that of the other three channels, most of the details in the image will come from the NIR pixels, whereas the RGB pixels can add to these details (especially in daytime) but will mainly add color to the image. To generate the full resolution 3D RGB image we first interpolate the NIR image, and then use it in the RGB interpolation process. After this interpolation, an additional image fusion step is performed in the HSI color space, between the NIR image and the intensity image produced by the transformation of the RGB image to HSI space.

The general image processing algorithm flow is:

- **FPN correction & linearization:** these are common processes that are performed in every image sensor. Their goal is to correct the sensor's Fixed Pattern Noise (FPN) and to improve uniformity throughout the full image dynamic range.
- **White Balance:** the purpose of this block is to remove the effect of the illuminant of the scene, which can cause the colors in the image to deviate, according to their temperature. In general, we wish to make grey objects appear grey in the image, after this step.
- **NIR image interpolation:** in this block we perform interpolation in order to retrieve the missing NIR pixels, using the existing NIR pixels. We use gradients to determine the interpolation direction. Some additional processing of the image is performed at nighttime, to add information from a low-exposure image to saturated regions.
- **RGB image interpolation:** the purpose of this block is to estimate the values of the missing R, G and B pixels and produce a full 3D RGB image. As the sampling of R, G and B planes is very sparse (mainly of R & B), we use the interpolated NIR image as well as the NIR interpolation direction map in the RGB interpolation process.
- **NIR-RGB image fusion:** In this block we produce a single 3D RGB image out of the NIR and RGB interpolated images, where the color of the scene is taken from the RGB image and the details from the NIR and RGB images are combined. Before the fusion we transform the RGB image into the HSI color space, and the fusion itself is done between the Intensity image and the NIR image, while the Hue and Saturation layers remain untouched in this process.
- **Color-artifacts reduction:** during the RGB interpolation process, many color artifacts are created, mainly surrounding edges. These kind of artifacts are very common in all RGB demosaicing algorithms, and in our case they are even more severe. The reason for this is the very low sampling rate of the color components, which leads to wrong estimations of the color, near its edges. The purpose of this block is to reduce these artifacts by filtering the difference between the color planes ((R-G) and (B-G)).
- **White Balance (WB) Gains Calculation:** In this block we calculate the white balance gains that will be applied to the next image in the white balance step. We search for white pixels in the image, based on the assumption that the white pixels are pixels with high values in all three colors (also called prefect reflector method). After finding the white pixels, we calculate their mean value in each color, and use the ratio between these means to calculate the required gains.
- **Color Correction Matrix (CCM) and Brightness adjustment:** the purpose of these two blocks is to make the final image more suitable for display purposes.

5. RESULTS

In the first phase of the development process both the NIR blocking filter and the NIR bandpass filter were deposited on top of blank Si wafers. This enables us to fine-tune the deposition process, based on the analyses of the spectral response, before integrating the sensors on imager wafers. This section presents the results of the reflectance measurements on blank wafers for both the NIR bandpass and the NIR blocking filter.

5.1 NIR BPF

The NIR bandpass filter was deposited on top of a blank Si wafer to enable the analyses of its FWHM and central wavelength. The reflectance of the filter was measured at the center and the edge of the wafer using collimated light. Therefore, the results are compared to the simulated reflectance of the nominal design for collimated light. The measured response of the filter shows a good fit both in terms of FWHM and central wavelength.

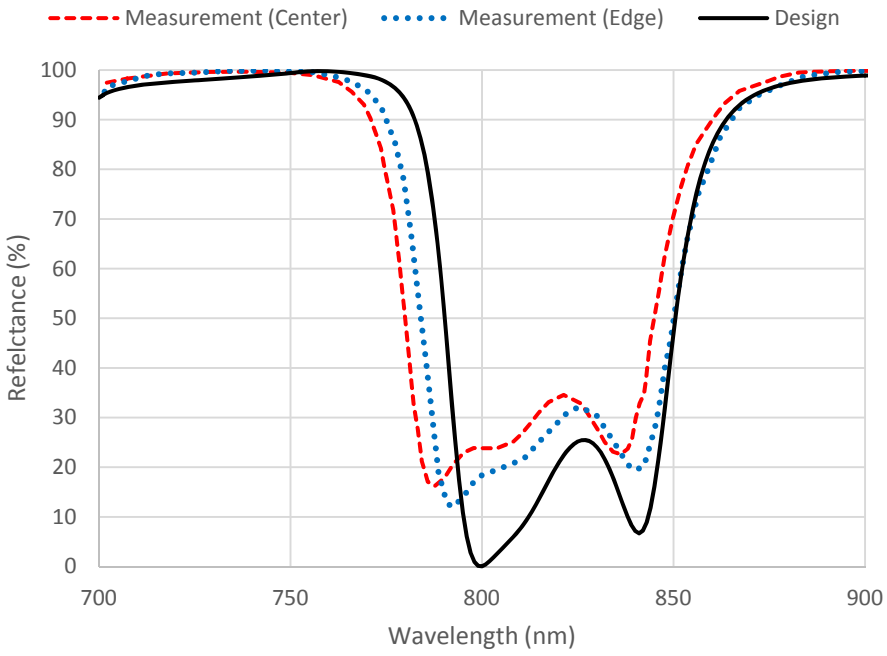

Figure 6: Reflectance as a function of wavelength for the NIR filter deposited on top of a blank wafer. The blue curve depicts the spectral response of the nominal design. The red and black curves correspond to measurements performed respectively on the edge and center of the wafer.

Table 4 gives an overview of the FWHM and central wavelength of the NIR bandpass filter for the different measurements. Note that the filters are not centered around 808 nm which is the central wavelength of the VCSEL module. This is due to the use of collimated light to measure the reflectance of the filter. This shift of the central wavelength counteracts the effect of the objective lens when the filters are implemented into the full system. From Table 4 one can see that the FWHM deviation is only 1.7 nm and 4.7 nm for respectively the measurement at the center and edge of the wafer. The shift on the central wavelength is 7.4 nm and 3.9 nm for respectively the measurement at the center and edge of the wafer. These shifts are well within 1 % of the targeted central wavelength.

Table 4: Comparing the NIR filter spectral performance of the nominal design with the measurement results at the center and edge of the wafer.

	FWHM	Central Wavelength
Nominal design	60.3 nm	820.4 nm
Measurement center	62 nm	813 nm
Measurement edge	65 nm	816.5 nm

5.2 NIR Blocking Filter

Figure 7 shows the reflectance as a function of wavelength for the measurements and the simulation of the nominal design of the NIR Blocking Filter. Again, the measurements were performed on the filter deposited on top of a blank Si wafer using an ellipsometer. This tool uses a normally incident collimated light bundle to measure the reflectance of the cutoff filter. The spectral range of this tool is limited to approx. 800 nm. The reflectance in the stopband and passband of the NIR blocking filter is in good agreement with the simulation of the nominal design on top of a Si blank wafer (black solid line). The spectral shift of the cutoff filter is approx. 7 nm which is within the specification of ±3 % of the edge wavelength.

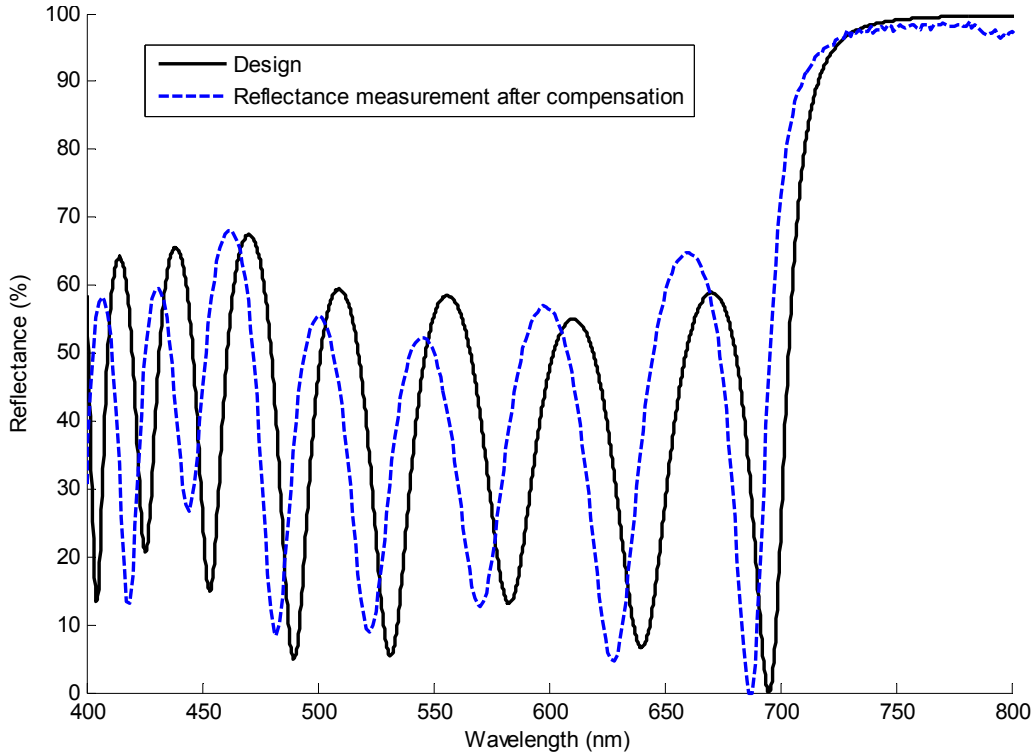

Figure 7: Reflectance as a function of wavelength for the nominal design (black) and the reflectance measurement for the compensated NIR blocking filter (blue dotted line).

6. CONCLUSION

We presented a RGB-NIR multi-spectral active gated imaging system addressing an integrated and cost-effective approach for low-light level and adverse weather conditions. We demonstrated the design and characterization of two novel custom spectral filters, which enable the parallel acquisition of standard RGB channels and an additional NIR channel, implemented on the GCMOS. These filters will be combined with standard absorption based RGB filters at a later stage of the project. When one wants to capture a wide field of view with a low f-number the designed NIR BPF should be robust towards variations on the angle of incidence of the light. The spectral performance of the designed filter was simulated and analysed when taking into account the system level aspects of the sensor. Afterwards the design and spectral response of the NIR blocking filters for the RGB pixels was demonstrated. The designed NIR blocking filter showed an OD of 2.3 at the central wavelength of the VCSEL module and an average transmission of 83.8 % when taking into account the objective lens. Afterwards the filters were characterized by measuring the reflectance of the filters deposited on top of blank Si wafers. The results show a good agreement both in terms of spectral position and absolute reflectance values between the simulated spectral responses and the experimentally observed responses. We also presented a novel approach for image reconstruction based on the NIR and visible signals. In summary, this paper has introduced the system level description, design and characterization results of key components for a novel RGB-NIR time gated CMOS imaging system. The system presents an integrated cost effective solution for all weather active gated imaging in the transportation, security and commercial sectors.

REFERENCES

[1] Burghartz, J. N., Graf, H. -., Harendt, C., Klingler, W., Richter, H., & Strobel, M. (2007). HDR CMOS imagers and their applications. 528-531.

[2] I-ALLOW website: http://www.i-allow.eu/

[3] O. David, N. S, Kopeika & B. Weizer, "Range gated active night vision system for automobiles", Applied Optics, Vol. 45, No. 28, 7248-7254(2006).

[4] H. Garten, Y. Grauer, Y. David, Y. Abramson & O. David, "Recent results of night time driving and automatic obstacle detection by AGIS technology", Vision 2012, Versailles, France, (2012).

[5] Y. Grauer, "Active gated imaging in driver assistance system", Advanced Optical Technologies, DOI 10.1515/aot-2014-0001, (2014).

[6] Y. Grauer & E. Sonn, "Active gated imaging for automotive safety applications", Proc. SPIE 9407, Video Surveillance and Transportation Imaging Applications 2015, 94070F (March 4, 2015).

[7] "TRUESENSE Sparse Color Filter Pattern", Semiconductor Components Industries, Publication Order Number AND9180/D (2014).

[8] N. Tack, A. Lambrechts, P. Soussan, L. Haspelslagh. "A Compact, high–speed and low-cost hyperspectral imager", Proc. SPIE 8266, Silicon Photonics VII (2012).

[9] B. Geelen, N. Tack, A. Lambrechts, "A Snapshot Multispectral Imager with Integrated, Tiled Filters and Optical Duplication", Proc. SPIE 8613, Advanced Fabrication Technologies for Micro/Nano Optics and Photonics VI (2013).

[10] B. Geelen, C. Blanch, P. Gonzalez, N. Tack. A. Lambrechts, "A tiny, VIS-NIR snapshot multispectral camera", Proc. SPIE 9374, Advanced Technologies for Micro/Nano Optics and Photonics VIII (2015).

[11] A. Lahav, A. Birman, D. Perhest, A. Fenigstein, Y. Grauer & E. Levi, "A global shutter sensor used in active gated imaging for automotive", International Image Sensor Workshop (IISW) 2015 (June, 2015).

[12] Y. Grauer, "Laser safety approach in driver assistance system", International Laser Safety Conference (ILSC®) 2013, Orlando, U.S.A, (2013).

[13] TFCalc, available at http://www.sspectra.com/

[14] V. Chikane & C. S. Fuh, "Automatic white balance for digital still cameras", Journal of Information Science and Engineering 22.3 497-509 (2006).

[15] C. Fredembach & S. Süsstrunk, "Colouring the near-infrared", Color and Imaging Conference. Vol. 2008. No. 1. Society for Imaging Science and Technology (2008).

[16] K. G. Nikolakopoulo, "Comparison of nine fusion techniques for very high resolution data", Photogrammetric Engineering & Remote Sensing, 74(5), 647-659 (2008).

[17] R. Ramanath & W. E. Snyder, "Adaptive demosaicking", Journal of Electronic Imaging, 12(4), 633-642 (2003).

[18] R. W. Schafer & R. M. Mersereau, "Demosaicking: color filter array interpolation", IEEE Signal Process, 22, 44-54 (2005).